Electronic Supplementary Information (ESI)

Palladium(II) and platinum(II) saccharinate complexes with bis(diphenylphosphino)methane/ethane: synthesis, S-phase arrest and ROS-mediated apoptosis in human colon cancer cells

Ceyda Icsel,[a] Veysel T. Yilmaz,*[a] Muhittin Aygun,[b] Buse Cevatemre,[c] Pinar Alper[d] and Engin Ulukaya[d]

[a]Department of Chemistry, Faculty of Arts and Sciences, Uludag University, 16059 Bursa, Turkey.
[b]Department of Physics, Faculty of Sciences, Dokuz Eylul University, 35210 Izmir, Turkey
[c]Department of Biology, Faculty of Arts and Sciences, Uludag University, 16059 Bursa, Turkey.
[d]Department of Medical Biochemistry, Faculty of Medicine, University of Istinye, 34010 Istanbul, Turkey

Corresponding Author:

Prof. Dr. Veysel T. Yilmaz
Department of Chemistry
Faculty of Arts and Sciences
Uludag University
16059 Bursa, Turkey

E-mail: vtyilmaz@uludag.edu.tr

Table S1 Crystallographic data and structure refinement for complexes **1**–**8**.

	1	**2**	**3**	**4**	**5**	**6**	**7**	**8**
empirical formula	$C_{39}H_{32}N_2O_7P_2PdS_2$	$C_{41}H_{36}N_2O_7P_2PtS_3$	$C_{64}H_{52}N_2O_6P_4PdS_2$	$C_{64}H_{52}N_2O_6P_4PtS_2$	$C_{40}H_{32}N_2O_6P_2PdS_2$	$C_{40}H_{32}N_2O_6P_2PtS_2$	$C_{66}H_{56}N_2O_6P_4PdS_2$	$C_{72}H_{70}N_4O_8P_4PtS_2$
formula weight	873.12	1021.93	1239.47	1328.16	869.13	957.82	1267.52	1502.41
crystal system	monoclinic	tetragonal	triclinic	triclinic	tetragonal	tetragonal	monoclinic	monoclinic
space group	$P2_1/n$	$I4_1/a$	$P\bar{1}$	$P\bar{1}$	$P\bar{4}2_1c$	$P\bar{4}2_1c$	$P2_1/c$	$P2_1/c$
a, Å	21.662(5)	37.9658(17)	11.1137(4)	11.1118(4)	15.4948(5)	15.7420(8)	12.053(2)	12.0410(6)
b, Å	17.152(2)	37.9658(17)	11.1173(8)	11.1453(4)	15.4948(5)	15.7420(8)	15.931(2)	15.8287(7)
c, Å	23.382(4)	12.1250(9)	13.1286(6)	13.1213(5)	18.9918(8)	19.1532(9)	17.923(2)	18.0559(9)
α, deg	90.00	90	76.066(5)	75.742(3)	90	90	90	90
β, deg	117.04(2)	90	66.277(4)	66.147(4))	90	90	102.841(13)	102.811(5)
γ, deg	90.00	90	85.214(4)	85.857(3)	90	90	90	90
V, Å^3	7738(3)	17477(2)	1441.17(14)	1439.74(10)	4559.7(4)	4746.4(5)	3355.3(8)	3355.7(3)
T, K	293(2)	293(2)	293(2)	293(2)	293(3)	293(2)	293(2)	293(2)
Z	8	16	1	1	4	4	2	2
ρ_{calc} (g cm^{-3})	1.499	1.554	1.428	1.532	1.266	1.340	1.255	1.487
μ (mm^{-1})	0. 722	3.477	0.560	2.675	0.610	3.152	0.482	2.307
F(000)	3552	8128	636	668	1768	1869	1304	1528
θ (°)	2.869-25.026	3.166-25.012	3.129-26.372	2.860-25.681	2.940-25.027	3.083-25.017	3.200-25.027	3.176-25.675
collected refls	23748	14104	12075	10635	8111	7421	9542	11914
data/ parameters	13573 /841	7687/333	5872/358	5463/358	3927/241	4085/150	5885/361	6314/413
goodness-of-fit	0.998	0.951	1.061	1.028	0.965	1.027	1.013	1.063
R_1 [I>2σ]	0.0765	0.0865	0.0485	0.0332	0.0457	0.0555	0.0629	0.0417
wR_2	0.1563	0.2224	0.1319	0.0781	0.1092	0.1545	0.1642	0.0898

Table S2 Temperature-dependent fluorescence emission titration data for the interaction of the complexes with FS-DNA.

Complexes	T(K)	K_{SV}(M^{-1}) x 10^{-4}	K_F(M^{-1}) x 10^{-4}	ΔG° (kJ/mol)	ΔH° (kJ/mol)	ΔS° (J/Kmol)
1	293	2.3	10.9	–28.3	–86.4	–198.1
	297	1.9	8.2	–27.5		
	300	1.6	5.4	–26.9		
3	293	3.6	37.0	–31.4	–37.8	–22.0
	297	3.1	34.7	–31.3		
	300	2.8	27.1	–31.2		
4	293	6.6	24.0	–30.3	–100.5	–239.6
	297	5.9	15.8	–29.3		
	300	5.2	10.5	–28.6		
6	293	1.4	5.2	–29.5	–75.8	–158.0
	297	1.2	3.7	–28.9		
	300	1.0	2.9	–28.4		
7	293	2.3	6.3	–26.9	–49.1	–75.7
	297	1.7	5.3	–26.6		
	300	1.4	4.2	–26.4		
8	293	1.8	4.6	–26.2	–144.6	–404.0
	297	1.5	2.6	–24.6		
	300	1.3	1.4	–23.3		

Table S3 Temperature-dependent fluorescence emission titration data for the interaction of the complexes with HSA.

Complexes	T(K)	K_{SV}(M^{-1}) x 10^{-4}	K_F(M^{-1}) x 10^{-5}	ΔG° (kJ/mol)	ΔH° (kJ/mol)	ΔS° (J/Kmol)
1	293	12.6	5.1	–32.2	–50.6	–62.9
	297	11.1	4.7	–31.9		
	300	9.9	3.4	–31.7		
3	293	10.6	16.7	–35.1	–51.3	–55.4
	297	9.8	13.2	–34.8		
	300	9.1	10.9	–34.6		
4	293	8.3	3.7	–27.4	–50.9	–80.3
	297	7.7	2.9	–27.1		
	300	7.2	2.3	–26.8		
6	293	3.8	2.5	–30.4	–71.8	–141.3
	297	3.2	2.0	–29.8		
	300	2.8	1.4	–29.2		
7	293	4.2	2.9	–30.7	–87.6	–194.1
	297	3.9	2.1	–29.9		
	300	3.1	1.4	–29.3		
8	293	4.3	3.5	–30.3	–93.5	–215.7
	297	3.9	2.8	–29.4		
	300	3.4	1.6	–28.8		

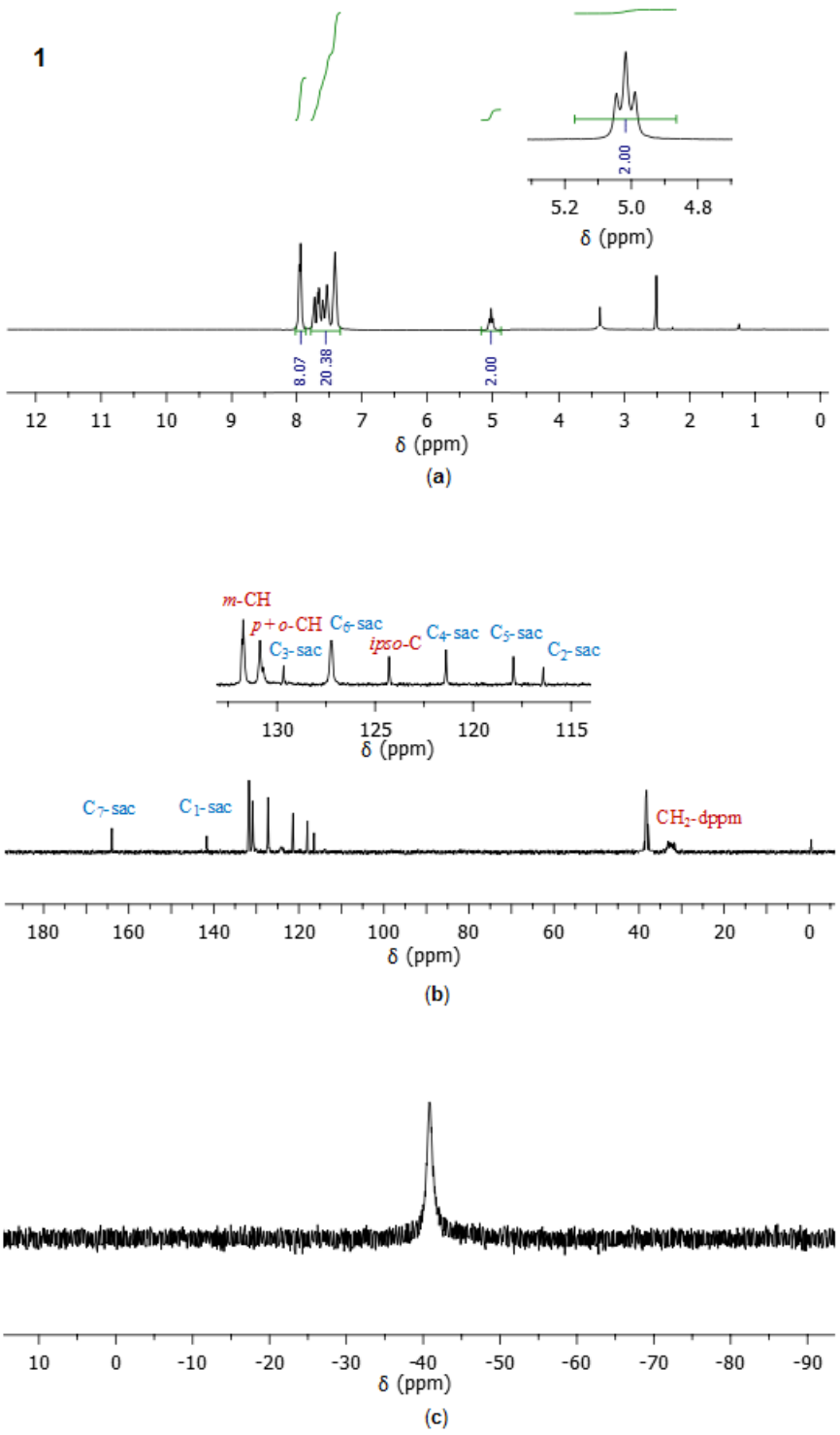

Fig. S1 continued

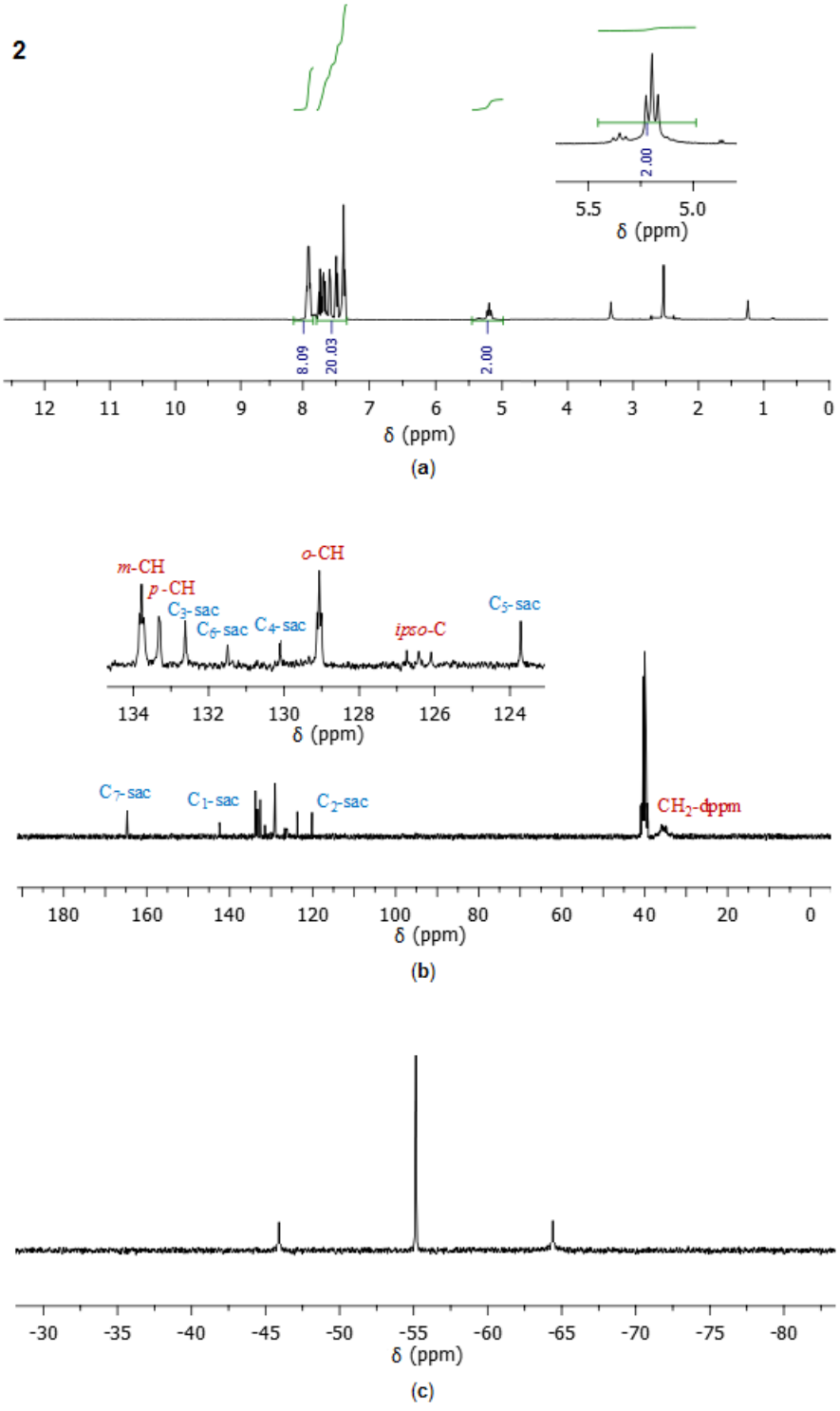

Fig. S1 continued

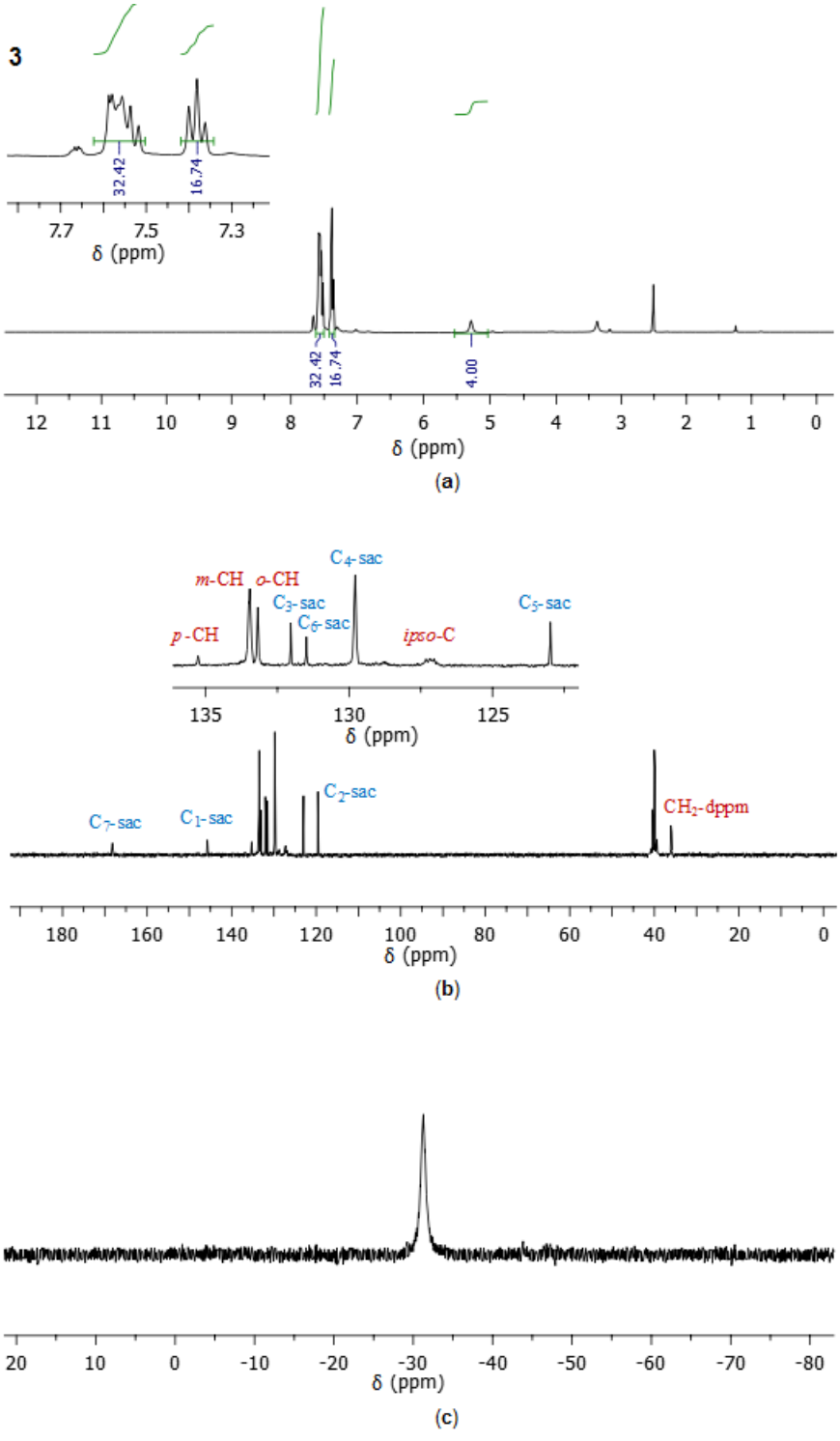

Fig. S1 continued

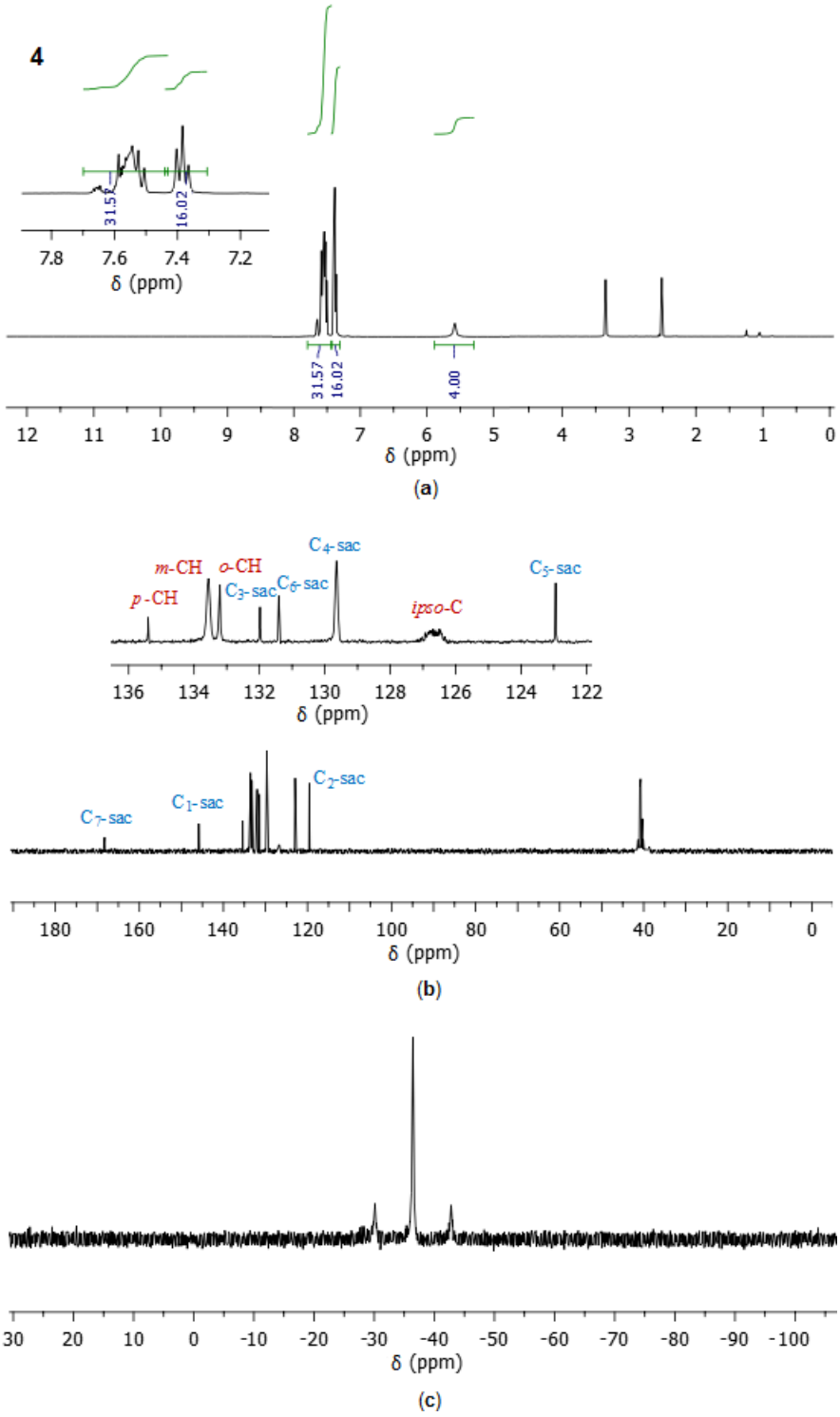

Fig. S1 continued

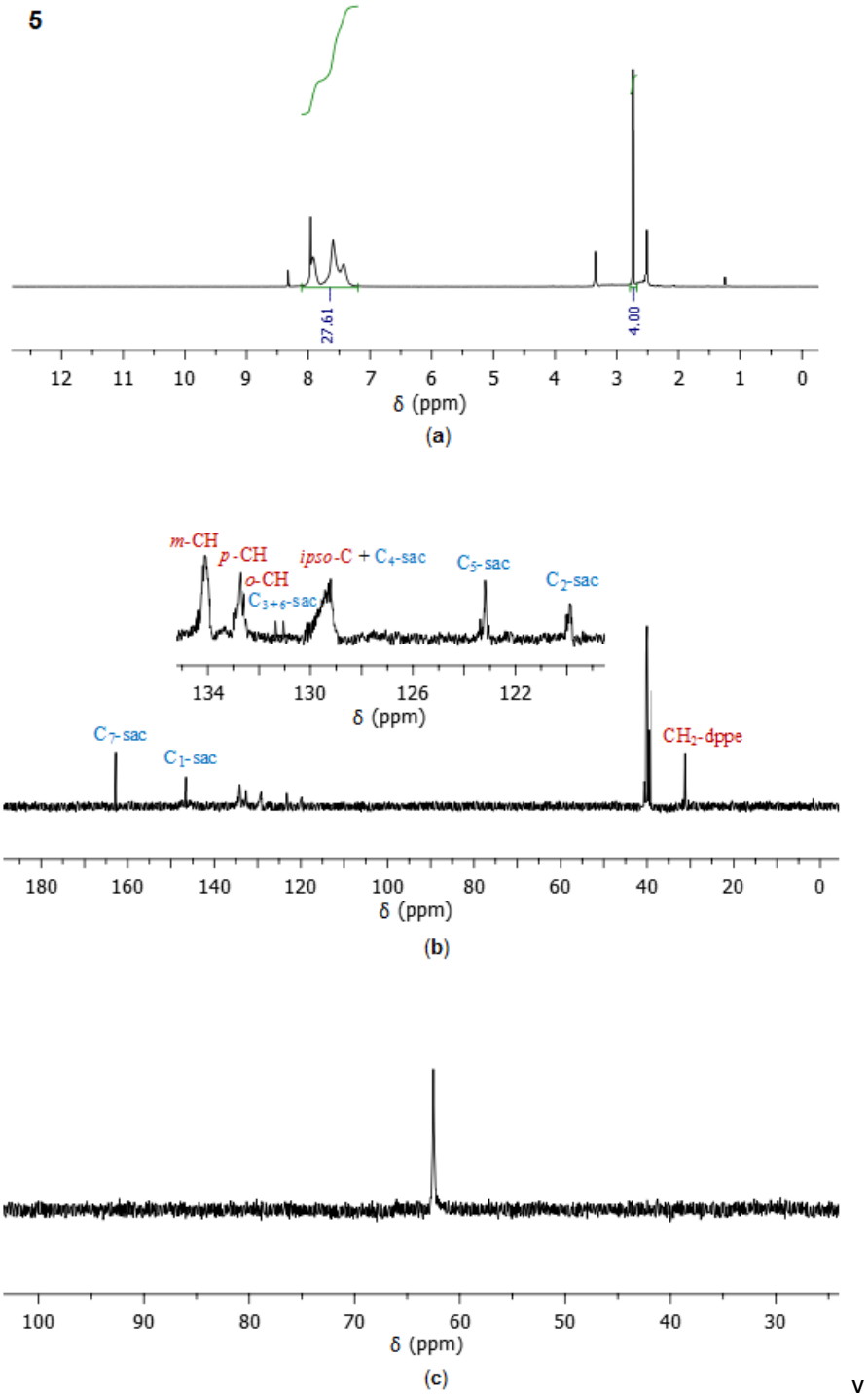

v

Fig. S1 continued

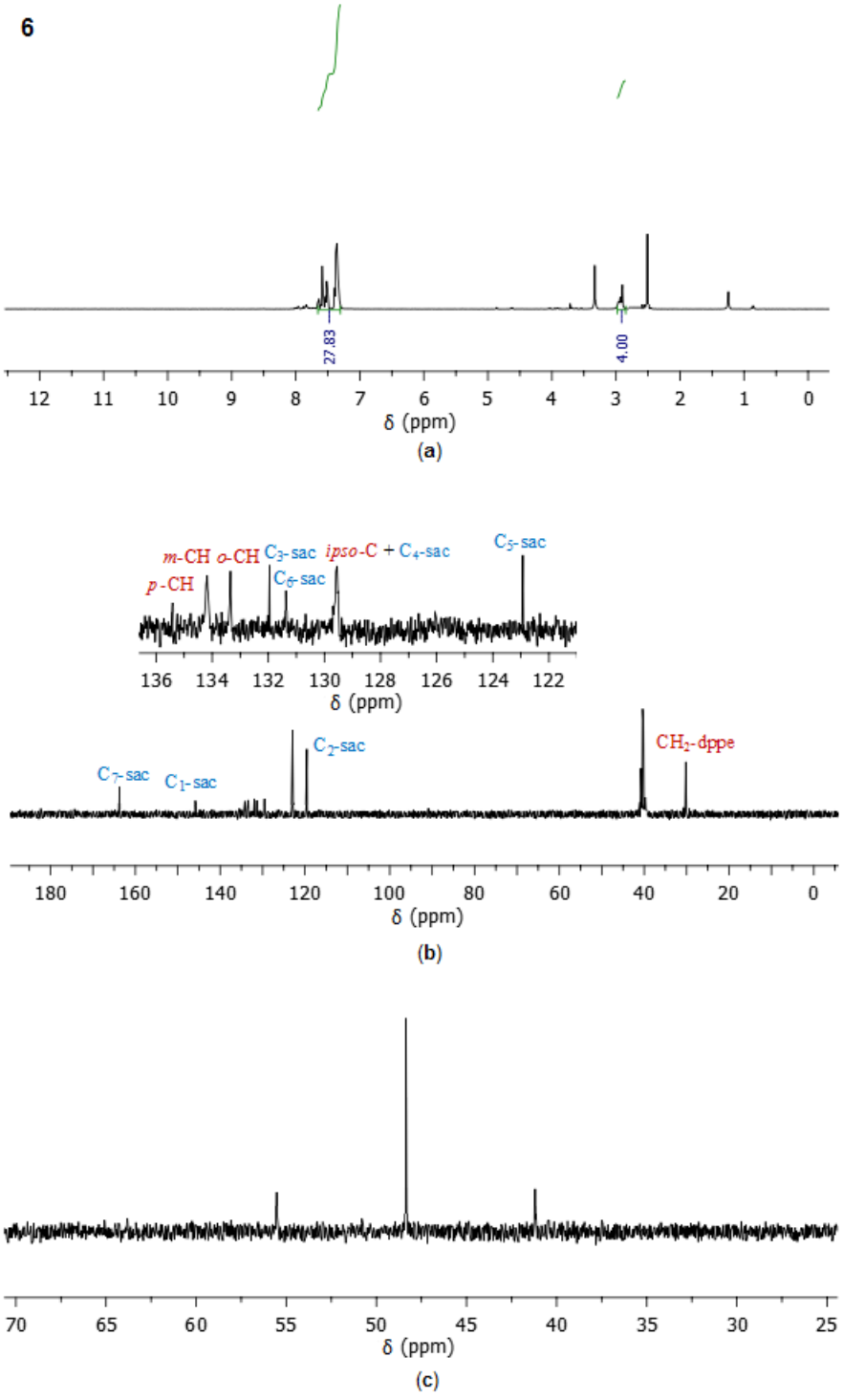

Fig. S1 continued

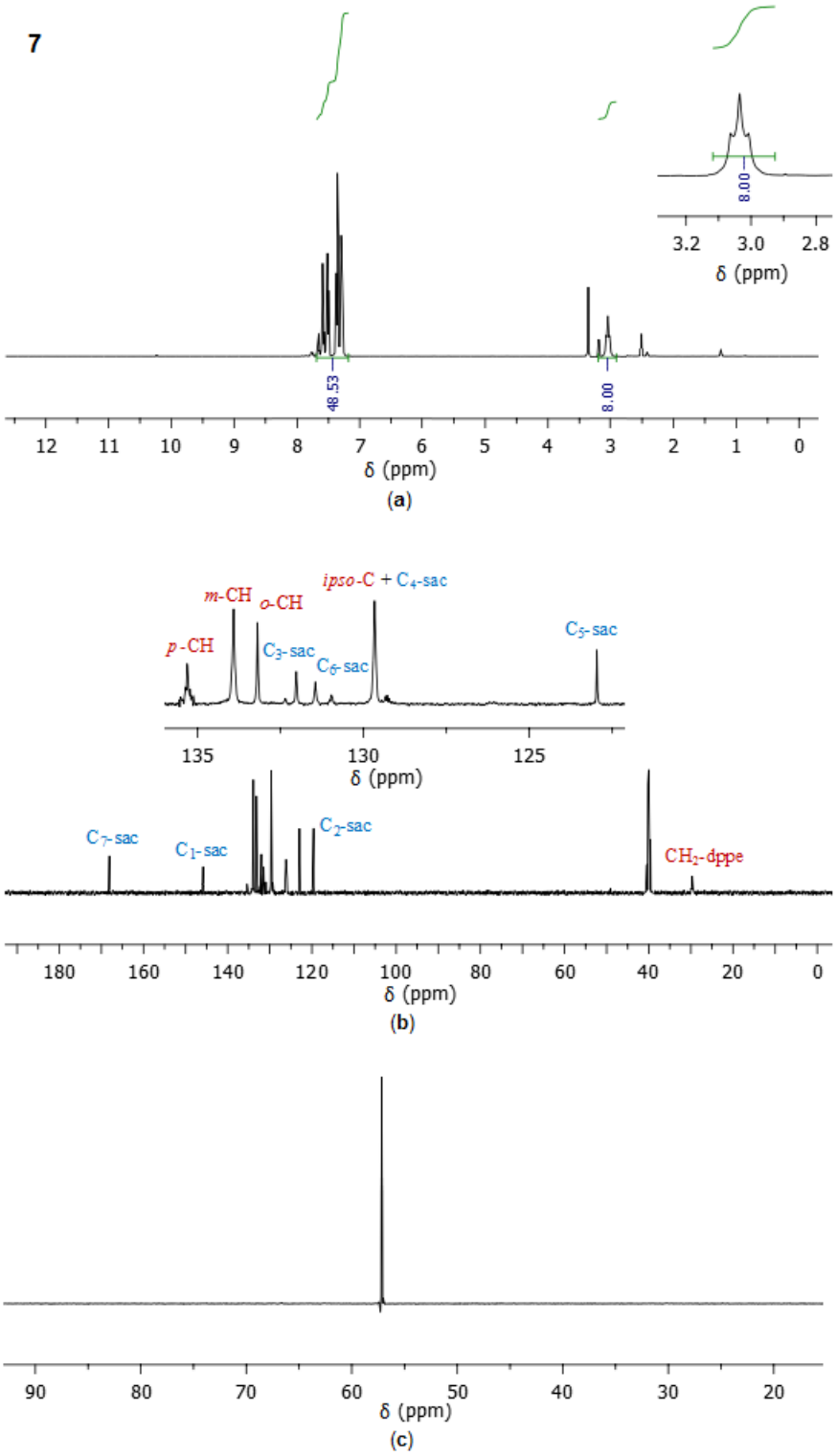

Fig. S1 continued

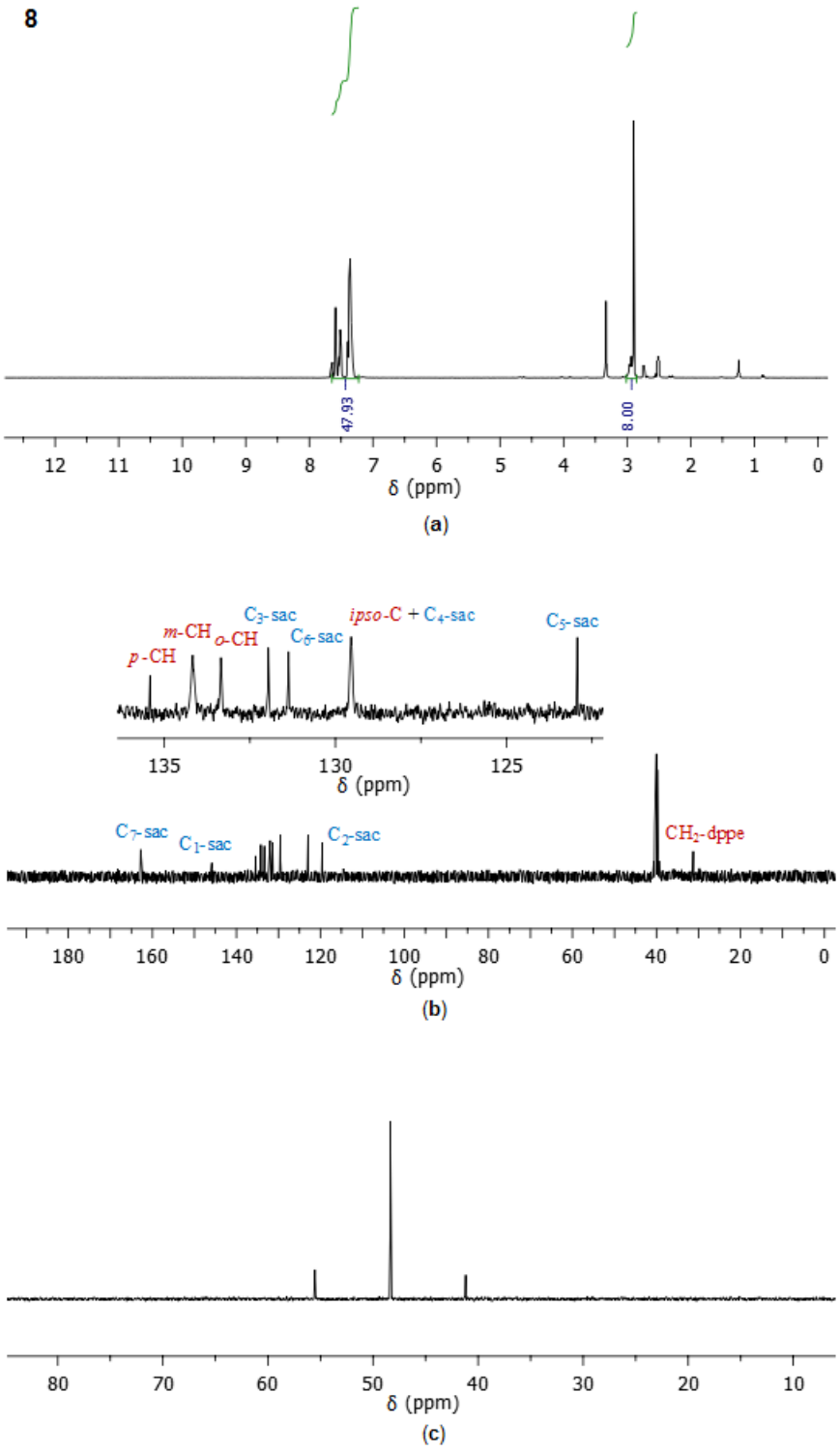

Fig. S1 ^{1}H- (**a**) ^{13}C- (**b**) and ^{31}P-NMR spectra (**c**) of **1**–**8**.

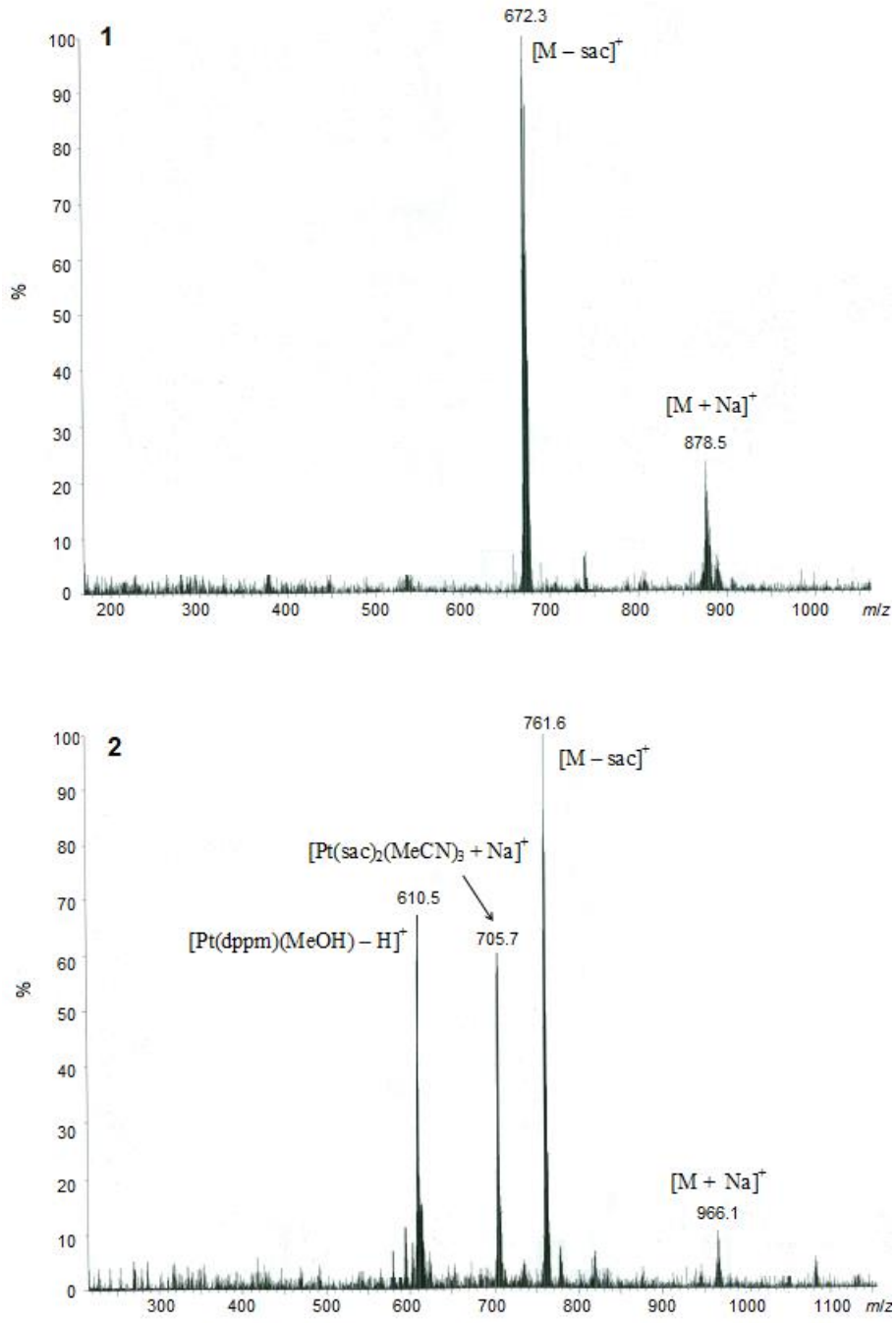

Fig. S2 continued

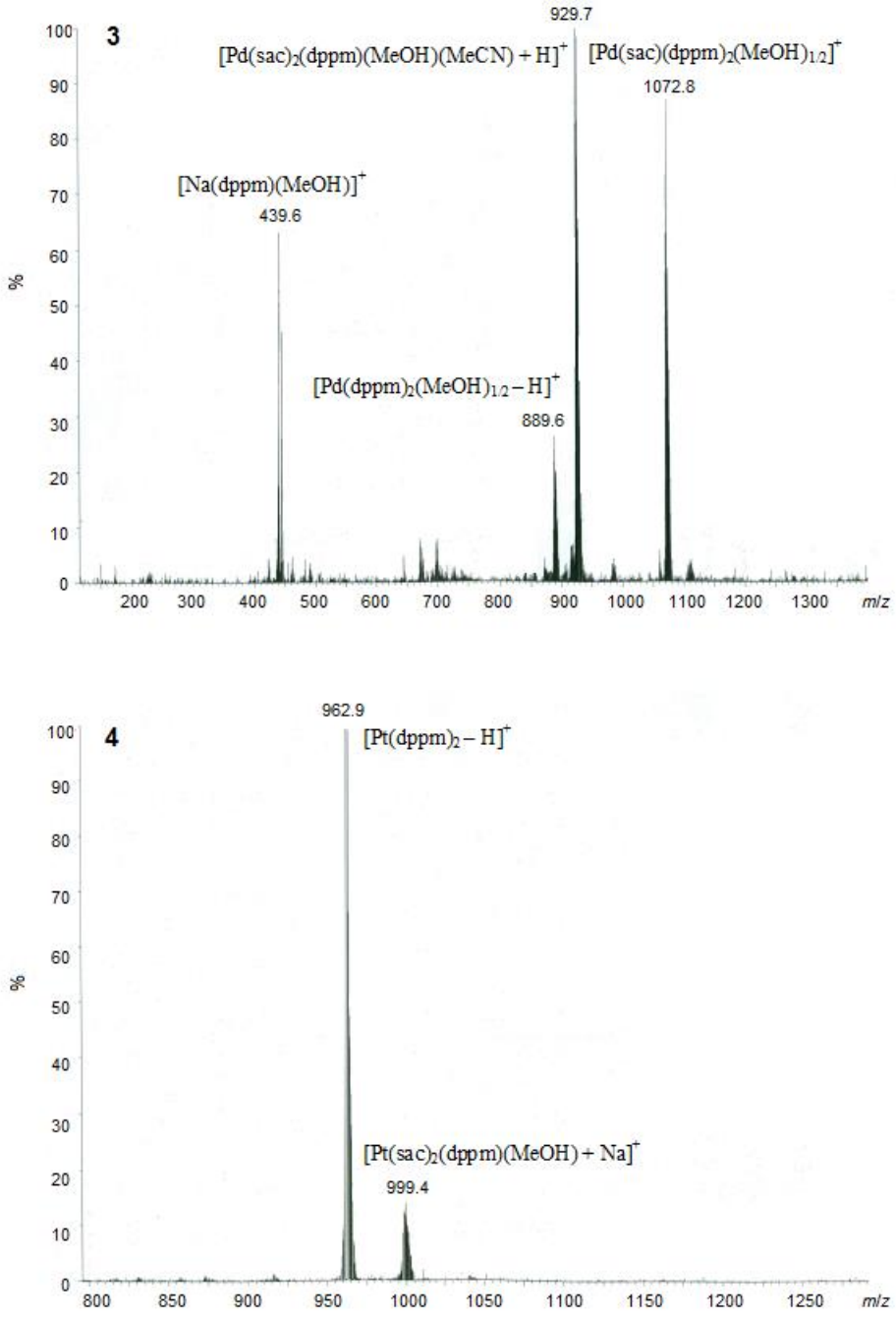

Fig. S2 continued

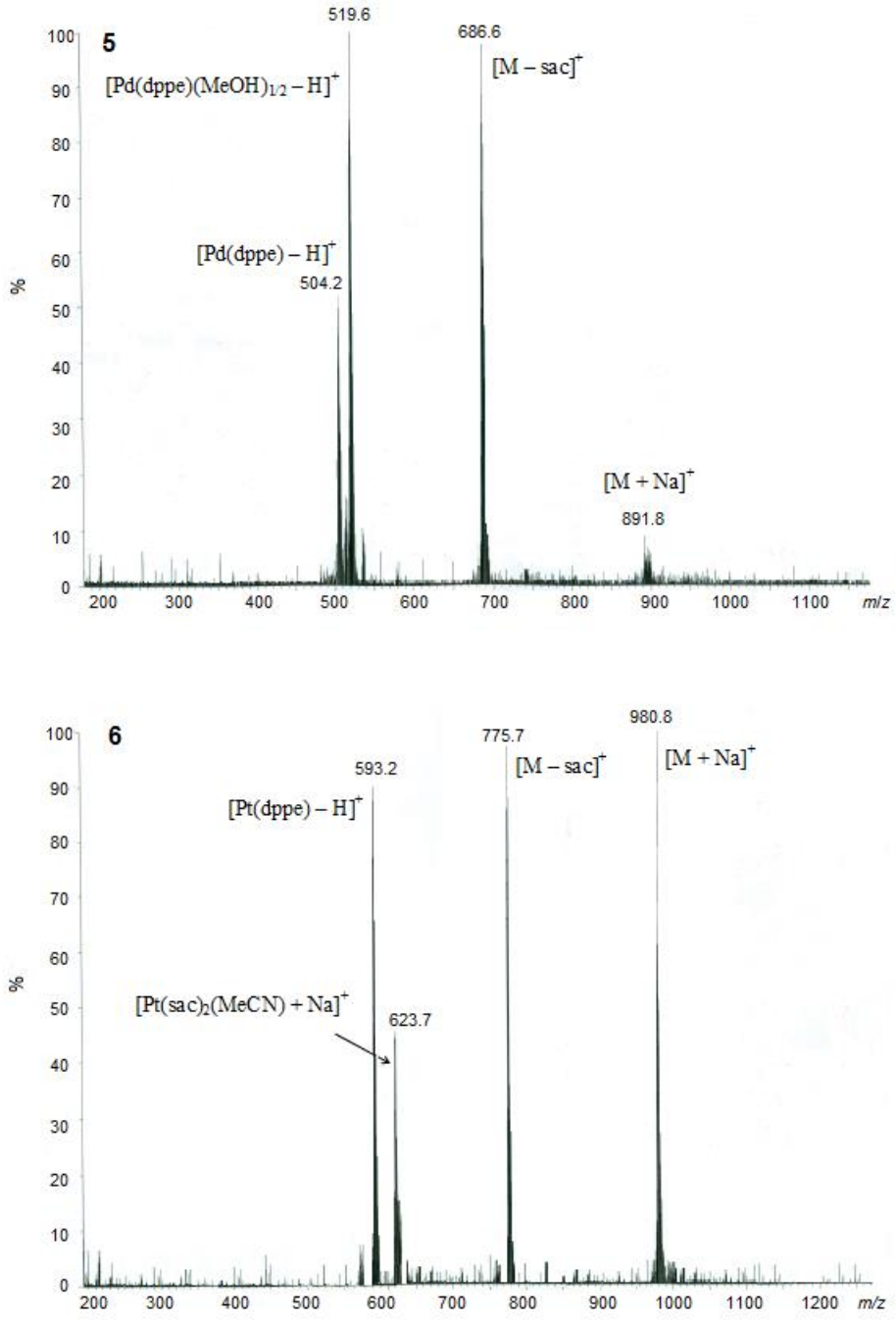

Fig. S2 continued

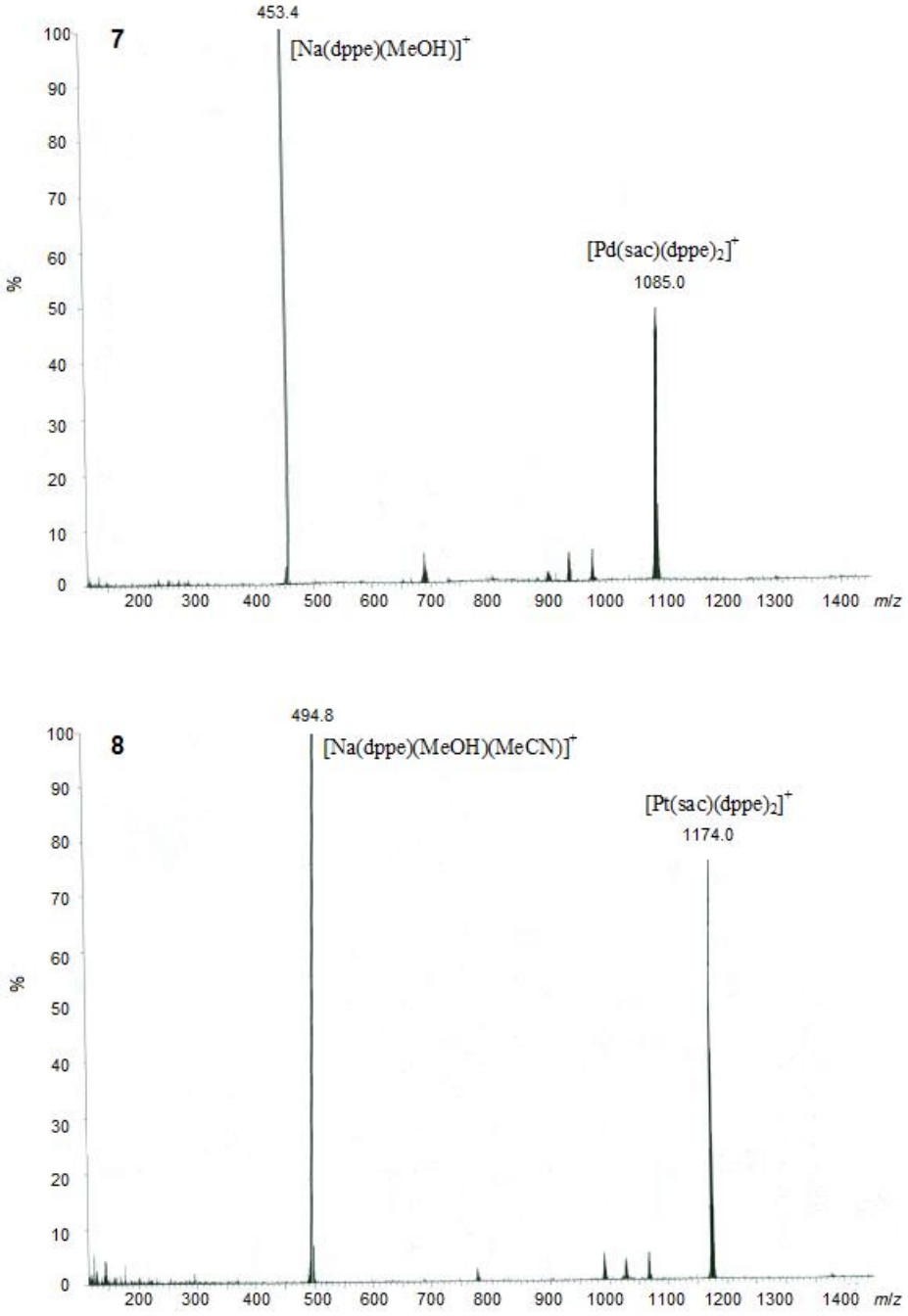

Fig. S2 ESI-MS spectra of **1**–**8**.

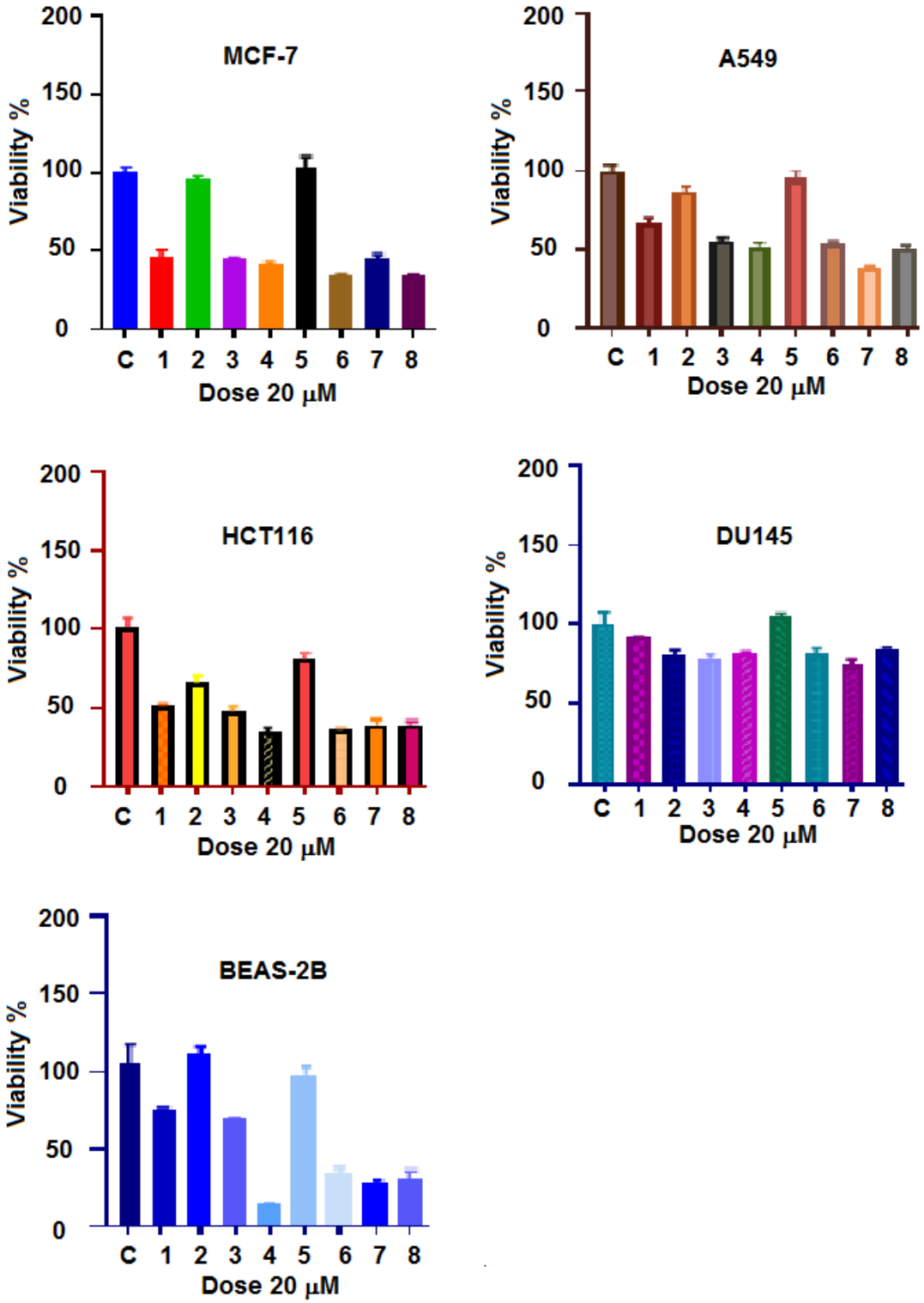

Fig. S3 The dose-response graphics for **1**–**8** obtained from SRB assay, showing the effect of the complexes (20 µM) on the growth of the cell lines after 48 h of treatment.

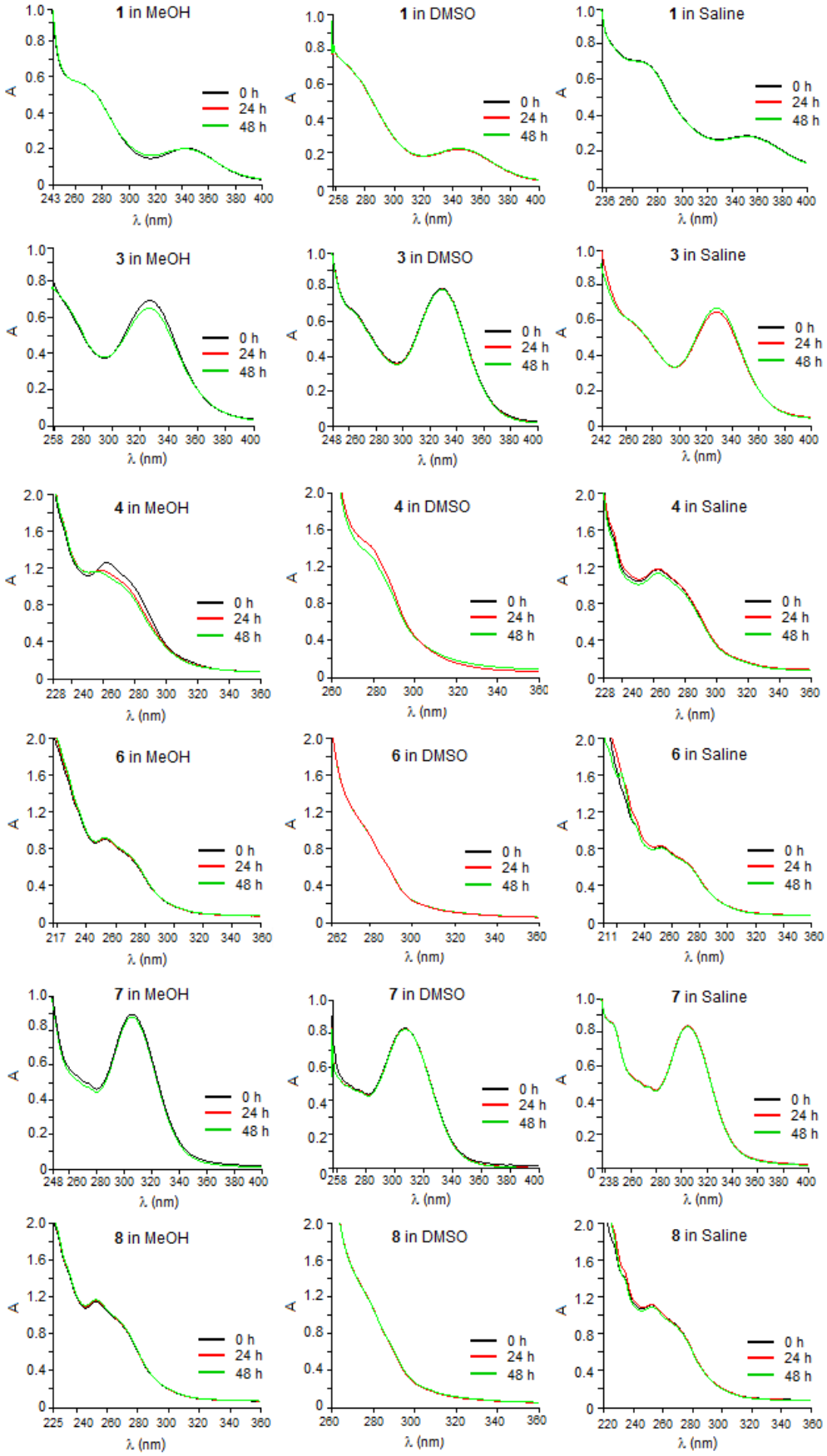

Fig. S4 UV spectra of the potent complexes, showing their stability in MeOH, DMSO and saline at 0, 24 and 48 h.

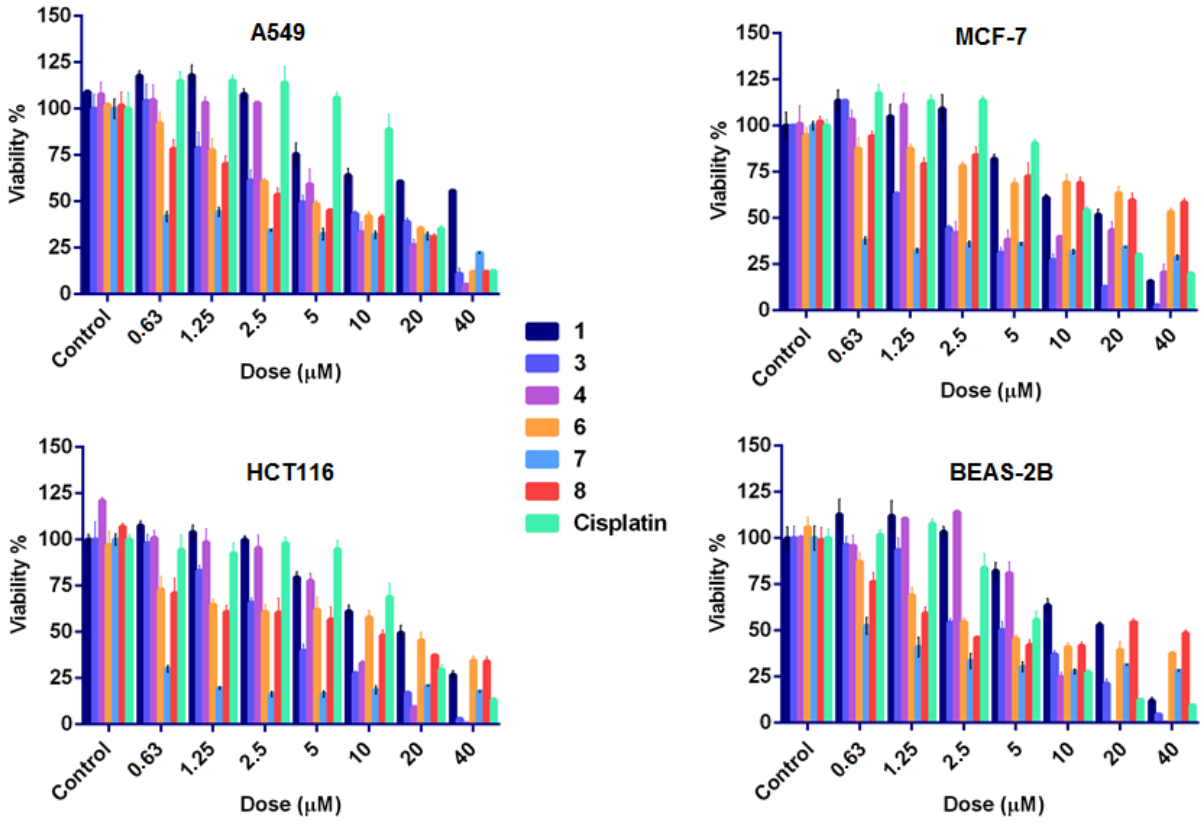

Fig. S5 The dose-response graphics for the potent complexes and cisplatin obtained from ATP assay, showing the effect of the complexes on the growth of the cell lines after 48 h of treatment.

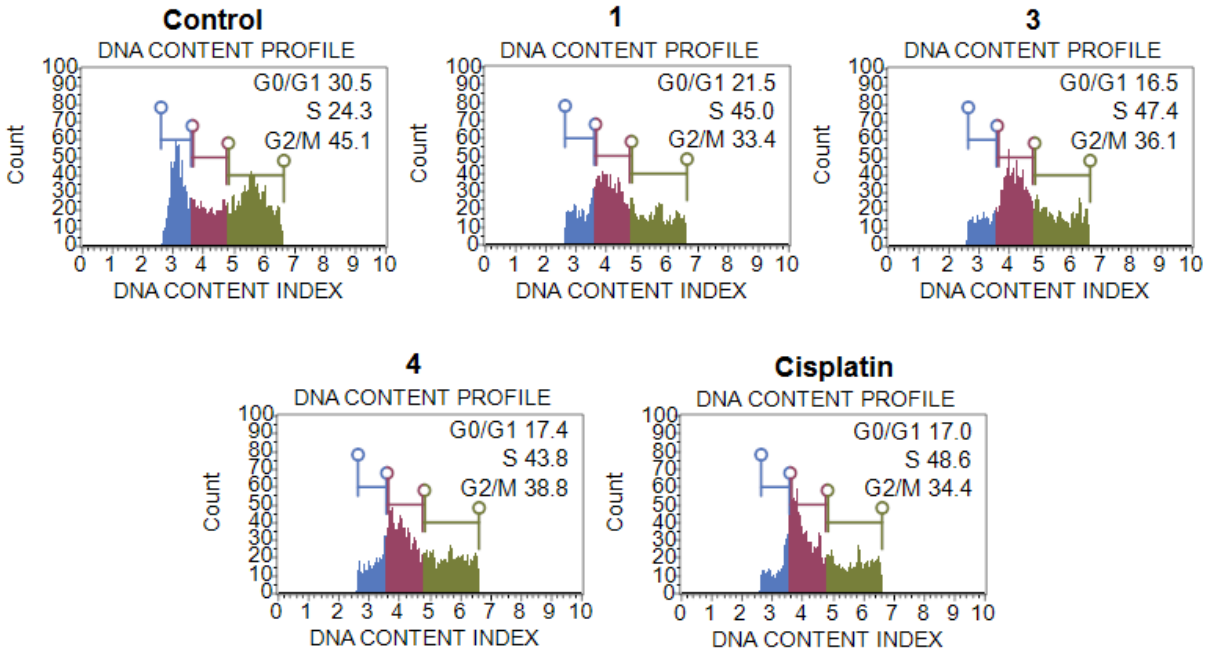

Fig. S6 Cell cycle progression of HCT116 cells treated with IC_{90} doses of **1** (50 µM), **3** (30 µM), **4** (20 µM) and cisplatin (44 µM) for 24 h.

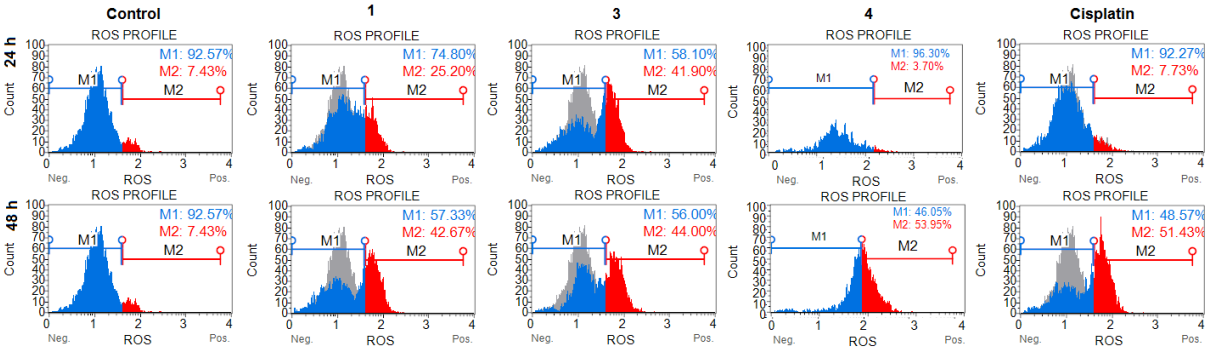

Fig. S7 ROS generation in HCT116 cells treated with IC_{90} doses of **1** (50 µM), **3** (30 µM), **4** (20 µM) and cisplatin (44 µM) for 24 and 48 h.

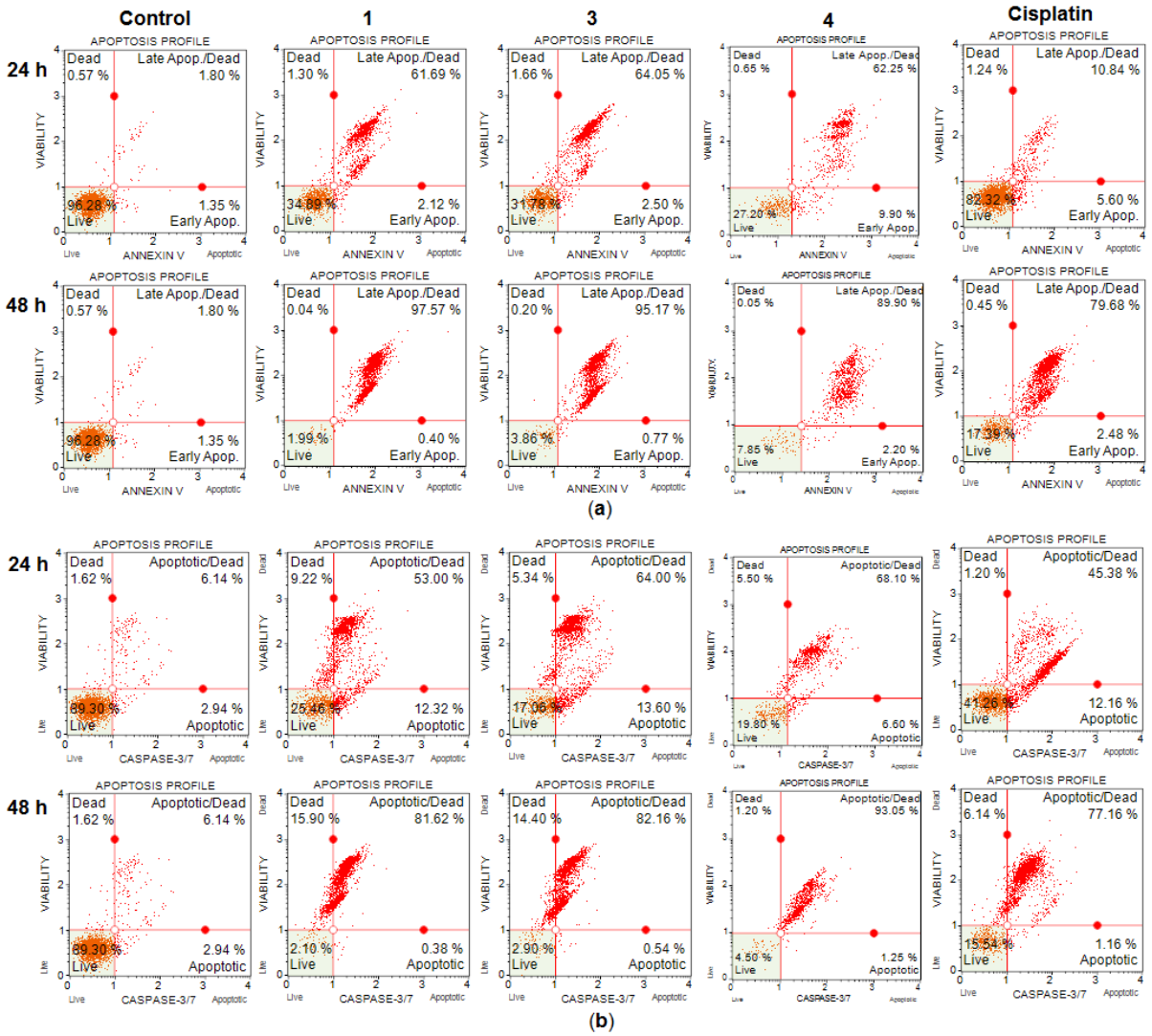

Fig. S8 (**a**) Annexin-V positivity and (**b**) Caspase 3/7 activity in HCT116 cells treated with IC_{90} doses of **1** (50 µM), **3** (30 µM), **4** (20 µM) and cisplatin (44 µM) for 24 and 48 h.

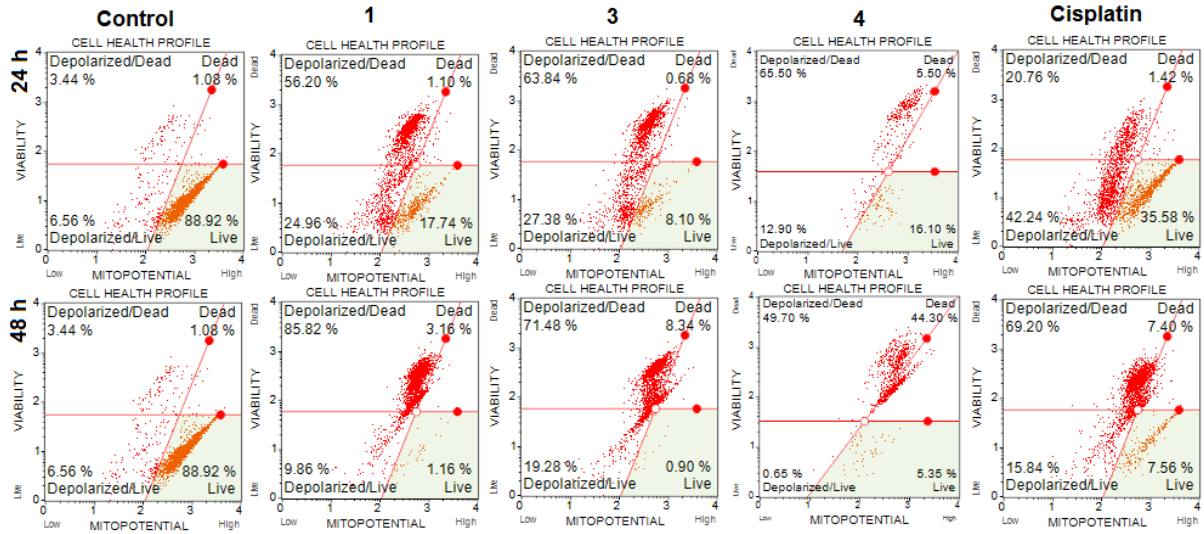

Fig S9 Mitochondrial membrane depolarization in HCT116 cells treated with the IC_{90} doses of **1** (50 µM), **3** (30 µM), **4** (20 µM) and cisplatin (44 µM) for 24 and 48 h.

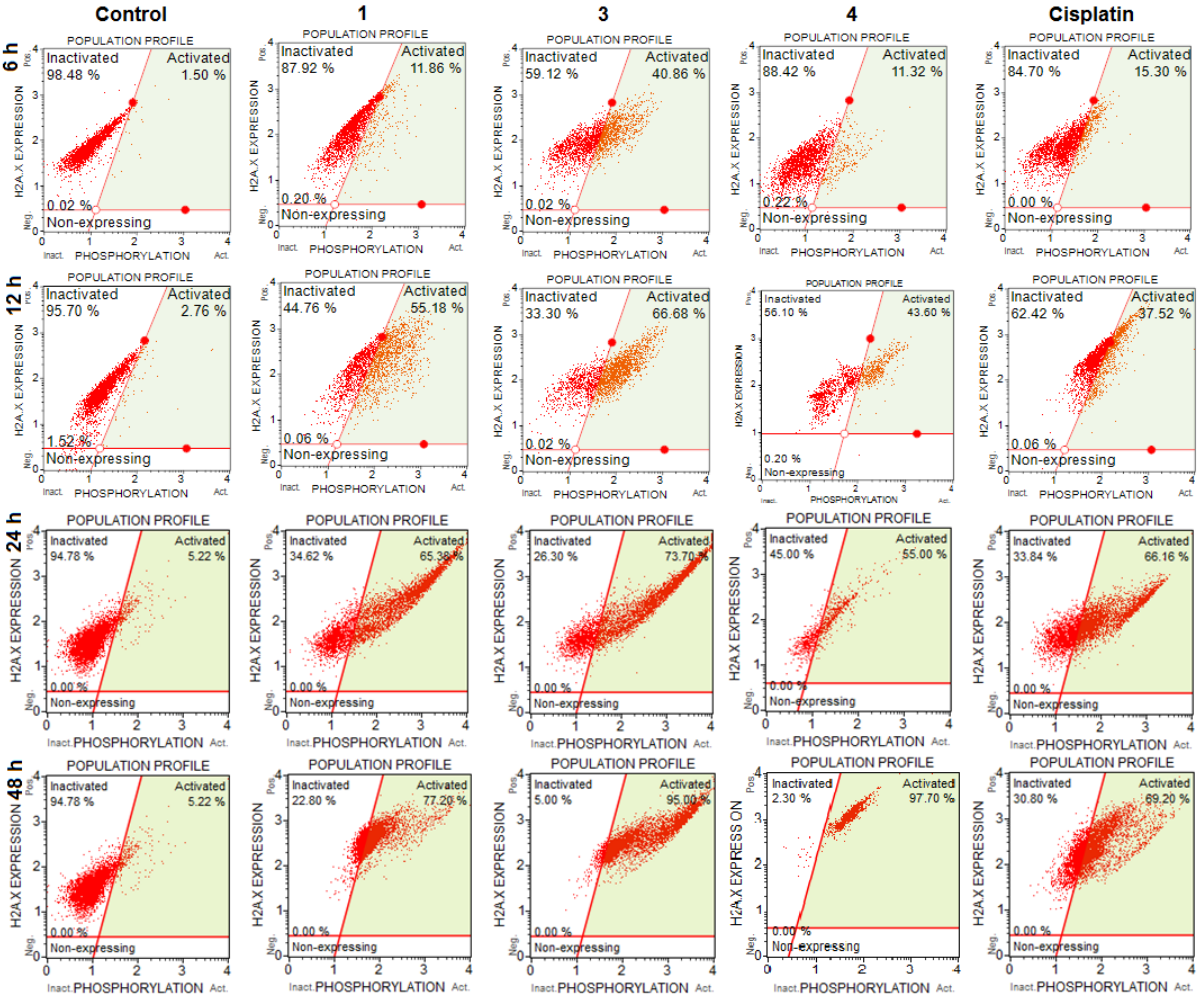

Fig S10 Formation of DNA double-strand breaks in HCT116 cells treated with the IC_{90} doses of **1** (50 µM), **3** (30 µM), **4** (20 µM) and cisplatin (44 µM) for 6, 12, 24 and 48 h.

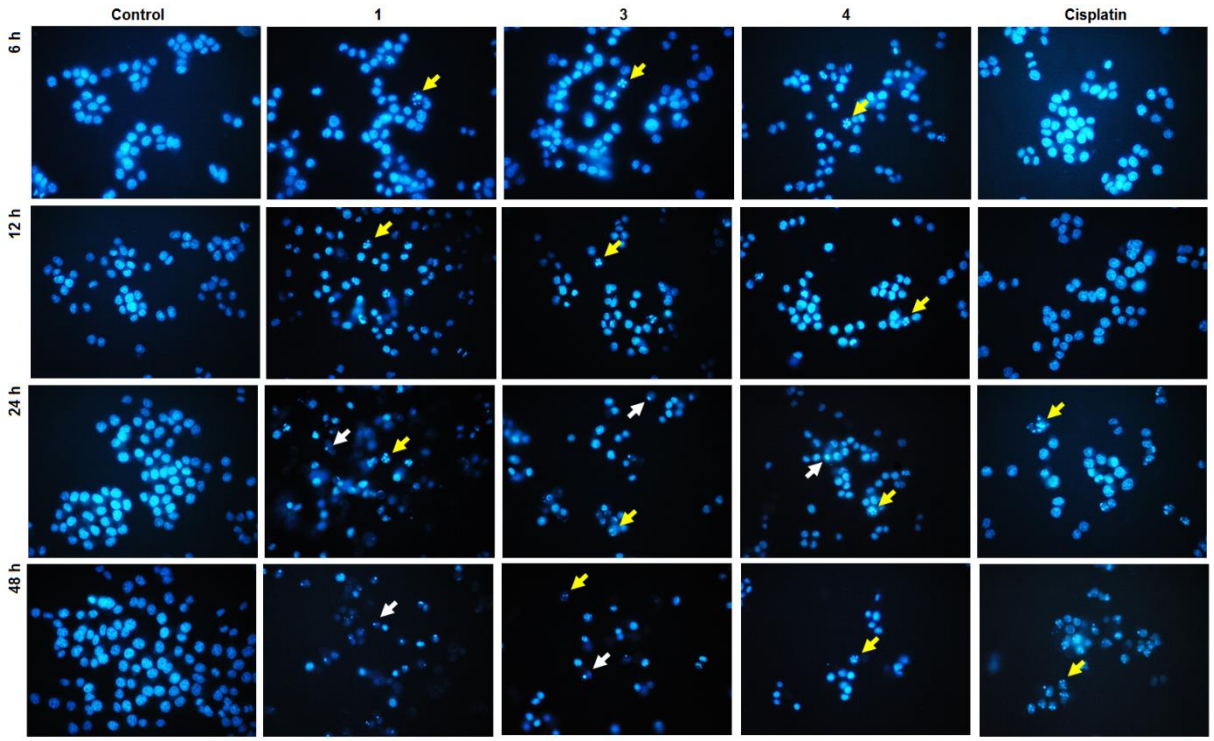

Fig. S11 Time-dependent morphological changes in the nuclei of HCT116 cells induced by the IC_{90} doses of **1** (50 μM), **3** (30 μM), **4** (20 μM) and cisplatin (44 μM). Cells were stained with Hoechst 33342 followed by detection using fluorescence microscope. Magnification: 40×.

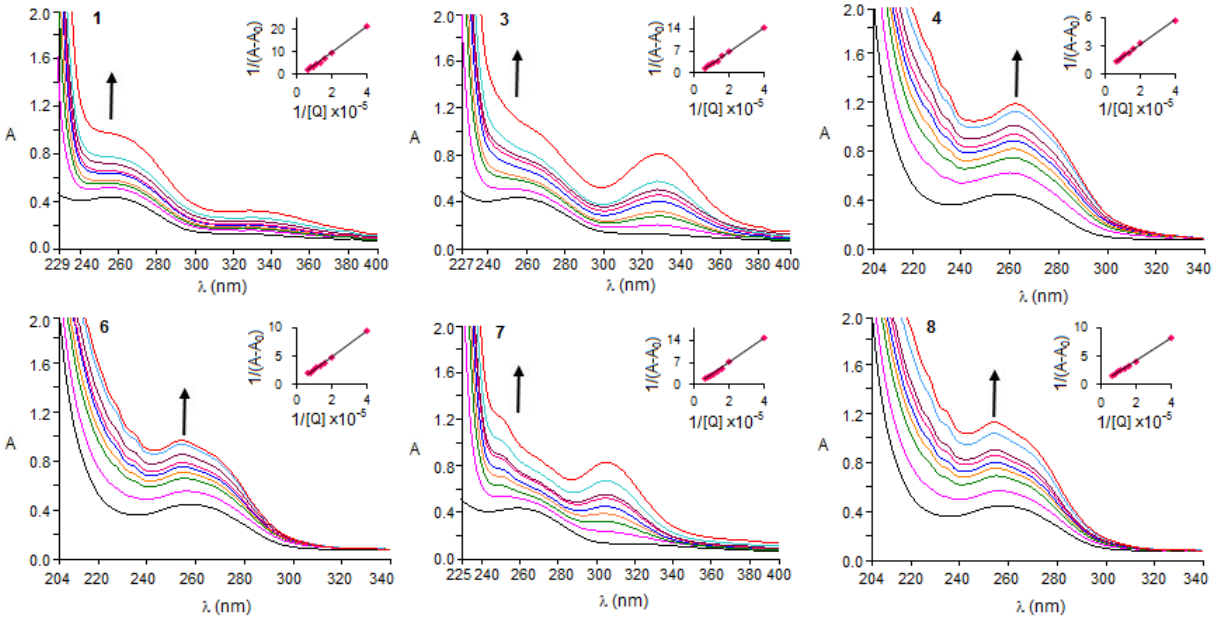

Fig. S12 Absorption titration spectra of FS-DNA solutions (50 µM) with increasing amounts of the potent complexes (0–15 µM) of in Tris-HCl buffer. Inset: plot of 1/[complex] vs. $1/(A–A_0)$.

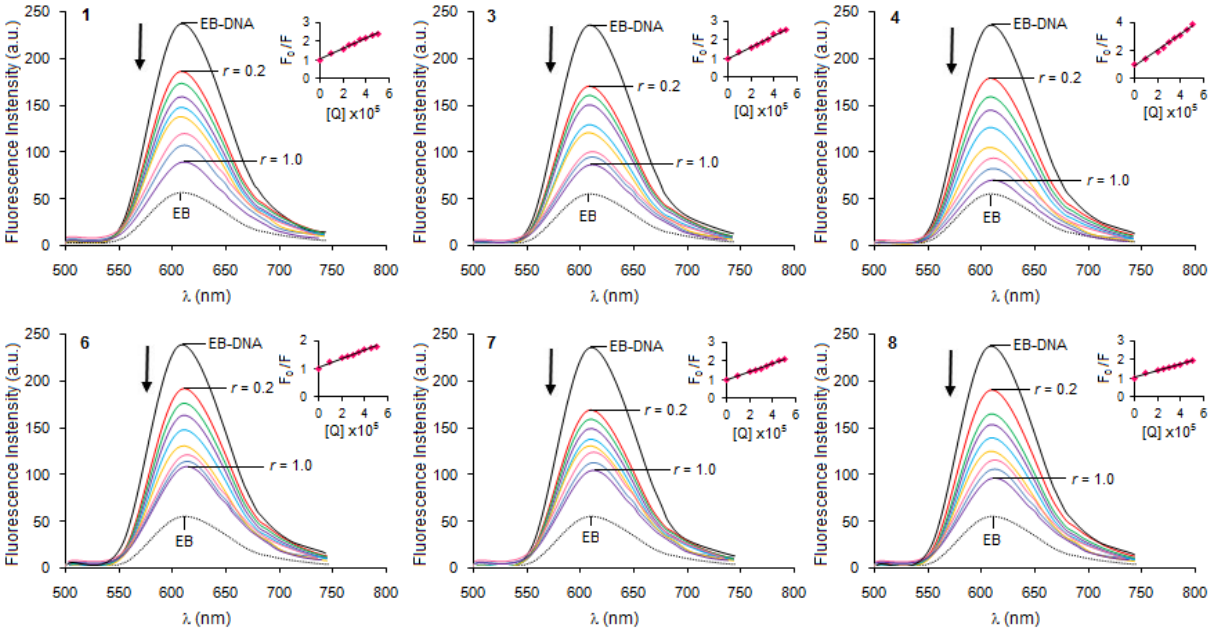

Fig. S13 Emission titration spectra of EB-bound DNA solutions in the absence and presence of increasing concentrations of the potent complexes (0–50 µM) in Tris-HCl. [EB] = 5 µM, [DNA] = 50 µM. The Inset shows the Stern-Volmer plot of the fluorescence data.

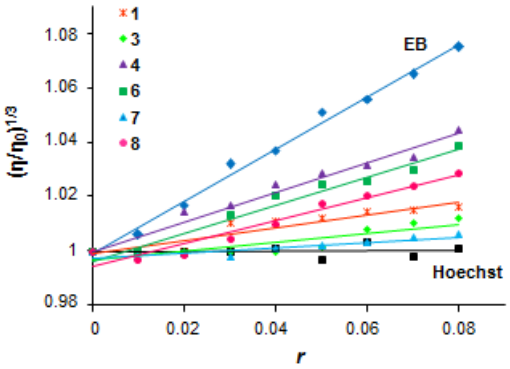

Fig. S14 The relative viscosity of FS-DNA (0.8 mM bp) upon addition of increasing amounts of the potent complexes, EB and Hoechst 33258 in Tris-HCl buffer. η is the viscosity of DNA in the presence of complex, and η_0 is the viscosity of DNA alone. r = [Complex]/[DNA(bp)].

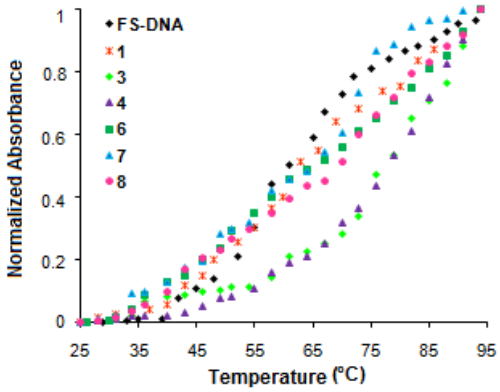

Fig. S15 Thermal denaturation profiles of FS-DNA (100 µM) in the absence and in the presence of the potent complexes (10 µM) in Tris-HCl.

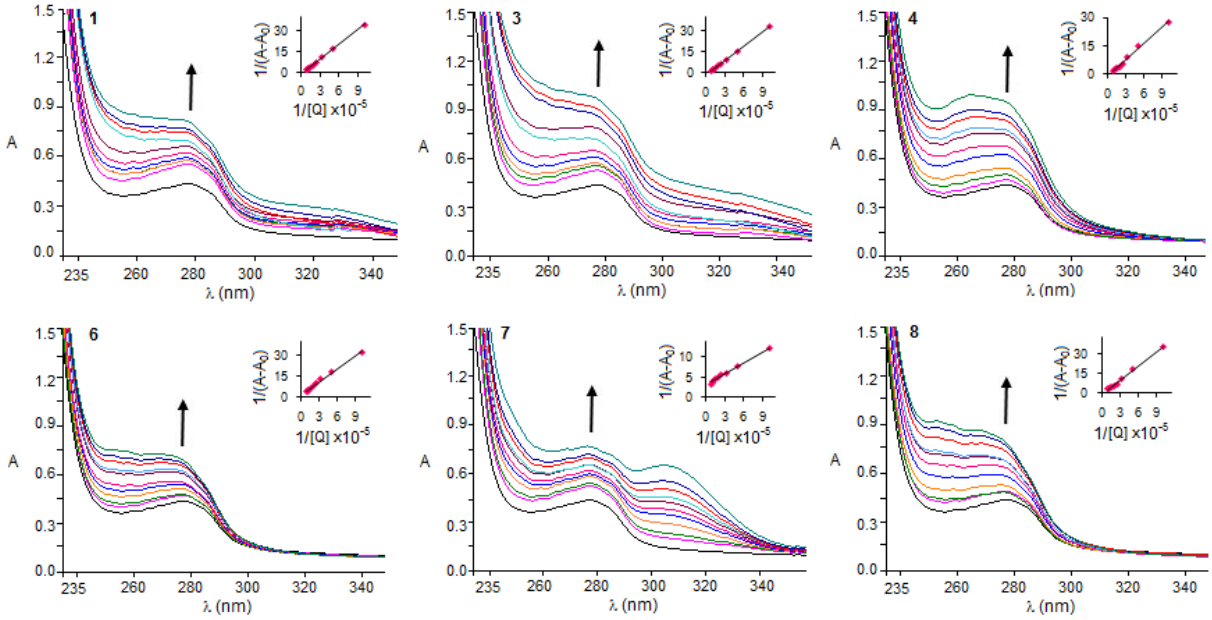

Fig. S16 UV absorption spectra of HSA (10 μM) upon addition of increasing amounts of the potent complexes (0–10 μM) in Tris-HCl buffer. The arrow shows the increases in absorbance. Inset: plot of 1/[complex] vs. $1/(A–A_0)$.

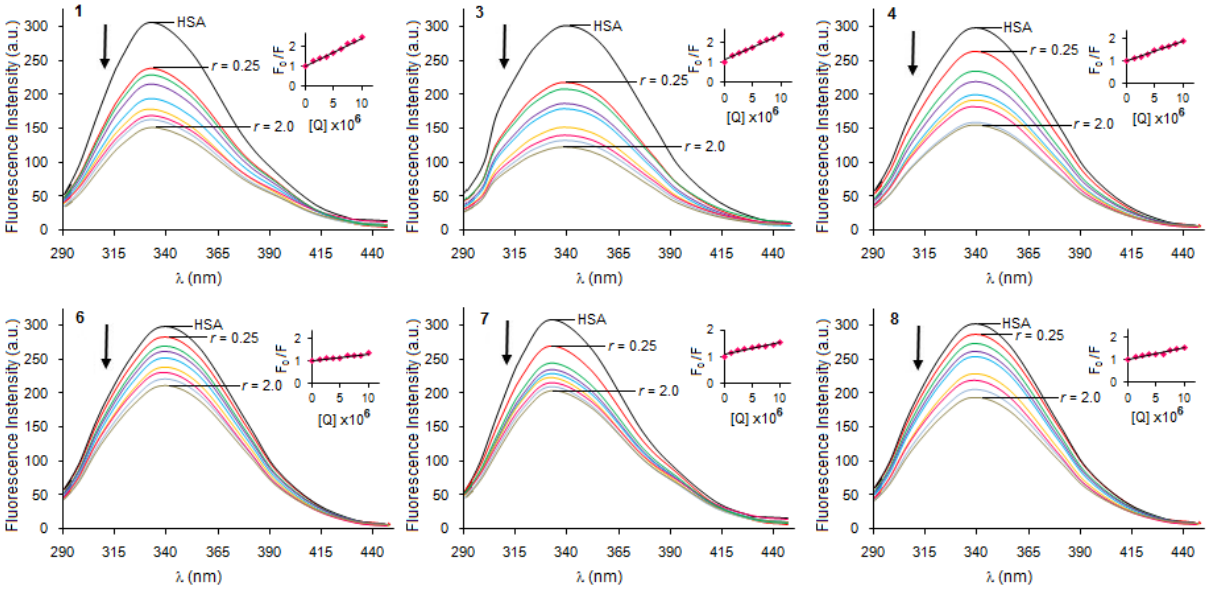

Fig. S17 Emission spectra of HSA (5 μM; λ_{ex} = 280 nm) in presence of the potent complexes (0-10 μM). The arrow shows the emission intensity changes upon increasing complex concentration. Insets: Stern-Volmer plot of the fluorescence data.

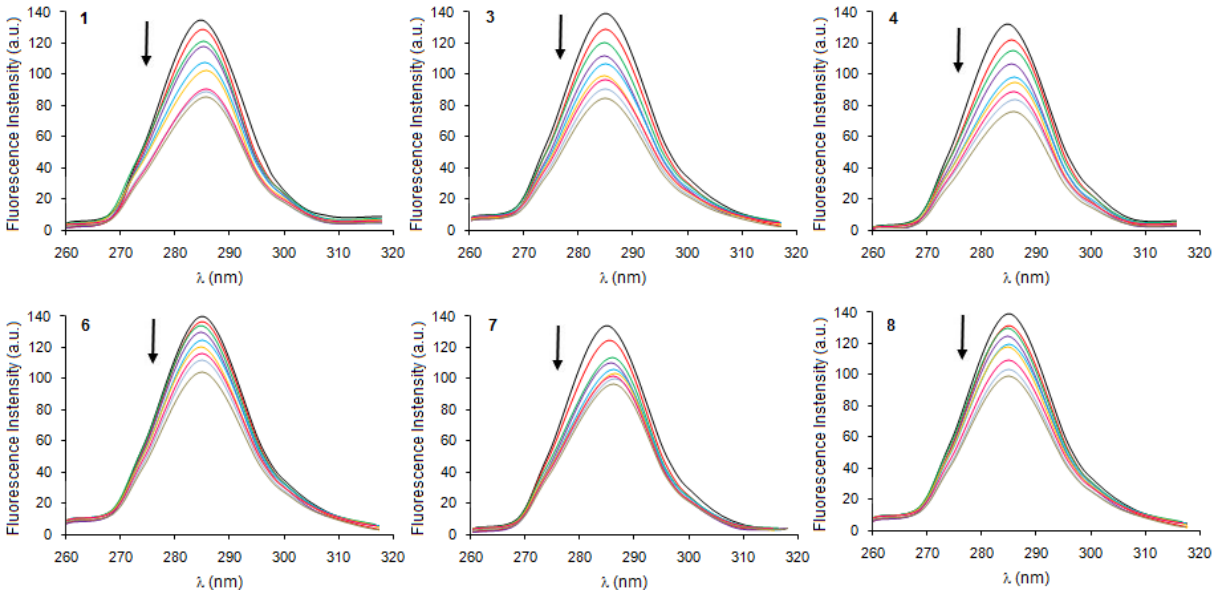

(**a**)

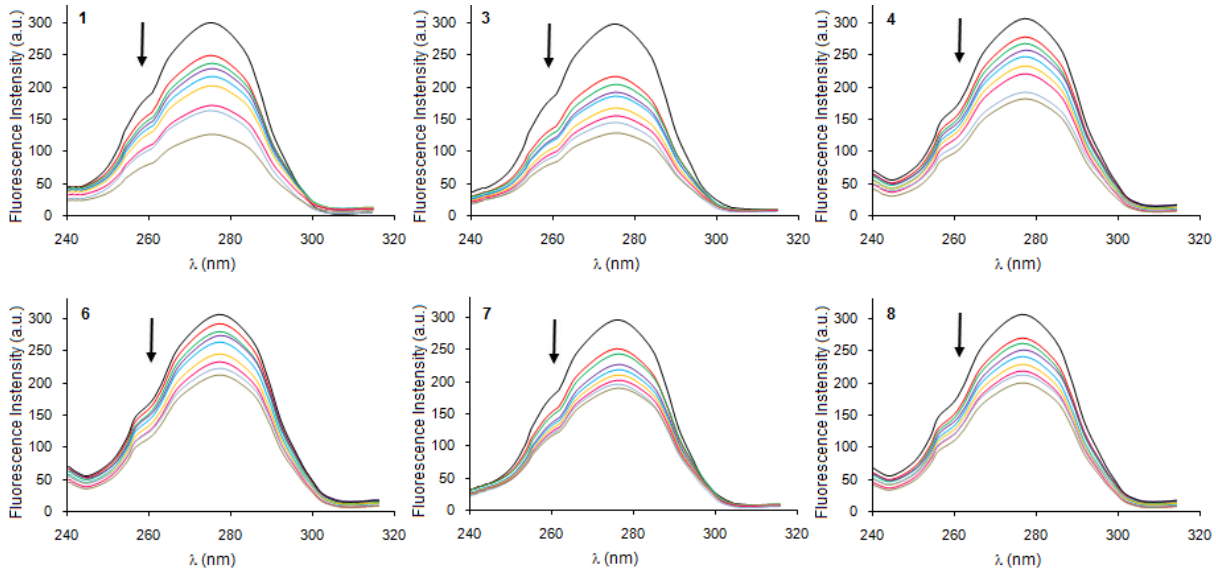

(**b**)

Fig. S18 Synchronous spectra of HSA (5 µM) in presence of the potent complexes (0-10 µM) at Δλ = 15 nm (**a**) and Δλ = 60 nm (**b**). Arrows show the emission intensity changes upon increasing concentration of the complexes.

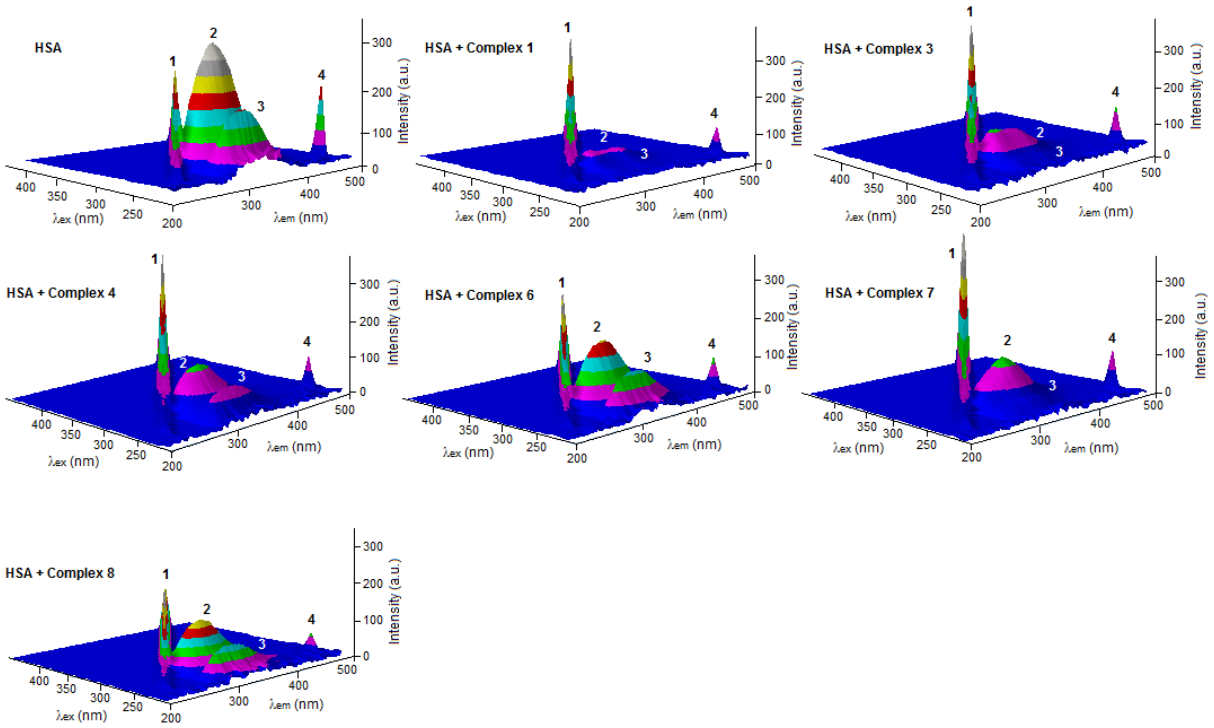

Fig. S19 3D fluorescence spectra of HSA (5 µM), and HSA (5 µM) + the potent complexes (5µM) in Tris-HCl buffer.